Angiogenesis (2019) 22:507–519
https://doi.org/10.1007/s10456-019-09675-z

ORIGINAL PAPER

PinX1 represses renal cancer angiogenesis via the mir-125a-3p/VEGF signaling pathway

Pingfu Hou[1,2] · Hailong Li[1,3] · Hongmei Yong[1,4] · Fang Chen[1,2] · Sufang Chu[1,2] · Junnian Zheng[1,2] · Jin Bai[1,2]

Received: 30 April 2019 / Accepted: 24 June 2019 / Published online: 28 June 2019

Abstract

Background PIN2/TRF1-interacting telomerase inhibitor 1 (PinX1) is a tumor suppressor in various tumors. However, the molecular mechanism underlying PinX1's role in cancer development and progression remains unclear. In this study, we aimed to uncover the new molecular mechanism and role of PinX1 in renal cell carcinoma (RCC) progression.

Methods We used miRNA microarray to detect the different expressed miRNAs upon PinX1 knockdown. Chromatin immunoprecipitation and Luciferase reporter assays were taken to identify the molecular mechanism of PinX1 in regulating mir-125-3p. In situ hybridization was performed to analyze the expression of mir-125a-3p in RCC using tissue microarray. The correlations between the mir-125a-3p expression level and clinicopathological features were evaluated using the χ^2 test. The role and molecular mechanism of PinX1 in RCC angiogenesis were investigated through a series of in vitro and in vivo experiments.

Results In this study, we discovered a new molecular mechanism of PinX1, in which PinX1 transcriptionally activated mir-125a-3p expression, thereby inhibiting the expression of vascular endothelial growth factor (VEGF), which is the target gene of mir-125a-3p. PinX1 also repressed tumor angiogenesis by increasing the mir-125a-3p expression in renal cancer. Moreover, the loss of mir-125a-3p expression was manifested in patients with RCC, and low miR-125a-3p levels correlated with poor survival of these patients.

Conclusions PinX1 represses renal cancer angiogenesis through mir-125a-3p/VEGF signal pathway. The miR-125a-3p may be a candidate clinical prognostic marker and a novel therapeutic target in RCC.

Keywords PinX1 · Angiogenesis · mir-125a-3p · VEGF

Electronic supplementary material The online version of this article (https://doi.org/10.1007/s10456-019-09675-z) contains supplementary material, which is available to authorized users.

Pingfu Hou, Hailong Li, and Hongmei Yong contributed equally to this work.

✉ Junnian Zheng
jnzheng@xzhmu.edu.cn

✉ Jin Bai
bj@xzhmu.edu.cn

[1] Cancer Institute, Xuzhou Medical University, 84 West Huaihai Road, Xuzhou 221002, Jiangsu, China

[2] Center of Clinical Oncology, Affiliated Hospital of Xuzhou Medical University, Xuzhou, China

[3] Department of Urology, Affiliated Hospital of Xuzhou Medical University, Xuzhou 221002, Jiangsu, China

[4] Department of Medical Oncology, Huai'an Hospital to Xuzhou Medical University, Huai'an, Jiangsu, China

Abbreviations

PinX1	PIN2/TRF1-interacting telomerase inhibitor 1
RCC	Renal cell carcinoma
IHC	Immunohistochemistry
ISH	In situ hybridization
TMA	Tissue microarray
OS	Overall survival
DFS	Disease-free survivals
VEGF	Vascular endothelial growth factor
ChIP	Chromatin immunoprecipitation
EMT	Epithelial–mesenchymal transition
MET	Mesenchymal–epithelial transition

Background

Globally, renal cell carcinoma (RCC) is one of the most common types of tumor in the urinary system. Although RCC death rate has decreased in the past two decades

because of prevention, early detection, and treatment, it still accounts for around 3% of human malignant tumor mortality [1]. Therefore, novel biological markers involved in RCC progression are needed to improve the diagnostic practices and to develop new therapeutic strategies for patients with RCC.

PinX1 was first identified in a yeast two-hybrid screen as a TRF1-binding protein and an endogenous telomerase inhibitor [2–4]. Moreover, PinX1 functions as a tumor suppressor, and its expression is frequently decreased in cancer tissues such as in breast cancer [5, 6], gastric cancer [7], ovarian carcinoma [8], bladder urothelial carcinoma [9], lymphoma [10], and renal cancer [11]. PinX1 can suppress tumor growth via telomere regulation [12] and promote moderate cell migration and invasion by suppressing MMP2 and MMP9 via NF-κB-dependent transcription [5, 11]. However, further investigation is needed to clarify the molecular mechanism underlying the role of PinX1 in cancer development and progression.

The abnormal regulation of miRNAs is associated with the presence of malignant tumor. The mir-125 family members play a role in different cancers, such as breast cancer [13], ovarian cancer [14], bladder cancer [15], liver cancer [16], and leukemia [17]. Vascular endothelial growth factor (VEGF) plays an essential role in the development, progression, and metastasis of malignant tumors, and it is a therapeutic target for treating various tumors [18]. mir-125a/b could repress VEGF expression to inhibit tumor growth and angiogenesis in different cancers, including hepatocellular carcinoma, ovarian cancer, and glioblastoma [19, 20].

In this present study, PinX1 functioned as a repressor of angiogenesis. At the molecular level, PinX1 transcriptionally activated mir-125a-3p expression, resulting in the repression of VEGF expression and inhibition of angiogenesis. Furthermore, mir-125-3p was overexpressed in patients with RCC, and it correlated with the clinicopathological parameters of such patients.

Methods

Cell lines and cell culture conditions

The RCC cell lines were obtained from the cell bank of Chinese academy of sciences. 786-O and ACHN cells were cultured in DMEM Medium supplemented with 10% fetal bovine serum, 100 U/mL penicillin, 100 μg/ml streptomycin, and incubated in a 37 °C humidified incubator with 5% CO_2.

Patients and sample collection

The tissue microarray (TMA) slide which included examination of 75 pairs of renal cancer tissues was purchased from Shanghai Outdo Biotech Company, and it included 75 patients who underwent Radical nephrectomy from 2006 to 2008. The TMAs including 307 RCC tissues were enrolled at Affiliated Hospital of Xuzhou Medical University from 2005 to 2008 in China. The patients' clinicopathologic information was obtained from the medical record of the Affiliated Hospital of Xuzhou Medical University. This study was conducted in compliance with the Declaration of Helsinki. Informed consent was obtained from all subjects. The ethics approval statements for human subjects were provided by the Ethnic Committee of the Affiliated Hospital of Xuzhou Medical University.

Western blot and antibodies

Western blot was performed as previously described [21]. Antibody against PinX1 (NBP2-32265; Novus Biologicals, LLC), GAPDH (sc-32233, Santa Cruz, Dallas, TX, USA), VEGF (19003-1-AP, Proteintech Group, Wuhan, China), E-cadherin (610181, BD Biosciences,), N-cadherin (610920, BD Biosciences), vimentin (550513, BD Biosciences), Fibronectin (610077, BD Biosciences), β-catenin (610154, BD Biosciences), and Occludin (33-1500, Life technology) were used for Western blot assays. Protein bands were detected by Tanon 5200 automatic chemiluminescence imaging analysis system using ECL reagent (Tanon, Shanghai, China).

Establishment of PinX overexpressing or knockdown stable cell lines

PinX1 overexpression and knockdown lentiviruses were purchased from Shanghai GenePharma Company. Stable cell lines overexpressing or lacking PinX1 were generated by being infected with lentivirus and selected with 2 mg/mL puromycin for about 2 weeks. Finally, the stable cell lines were verified using western blot.

Immunohistochemistry (IHC) and in situ hybridization (ISH)

IHC assays were performed as previously described [22]. For primary antibody incubation, anti-PinX1 antibody was applied at 1:100 dilution, anti-VEGF (19003-1-AP, Proteintech Group, Wuhan, China) antibody at 1:100 dilution, and anti-CD31 (11265-1-AP, Proteintech, China) antibody at 1:50 dilution. For in situ hybridization, DIG-labeled miRNA probes used for quantifying the expression of miR-125a-3p were purchased from the Exonbio Lab (Guangzhou, China). ISH was performed according to the protocol of the miRNA hybridization detection kit (D-2204B, Exonbio Lab, Guangzhou, China). Briefly, the tissue microarray blocks were deparaffinized, dehydrated, and subsequently treated with

Proteinase K Hybridization of DIG-labeled probes, which was done overnight at 42 °C. After stringency washes, the slides were incubated for 1 h with anti-DIG antibody, and at last the slides were incubated with DAB.

Immunofluorescence

Immunofluorescence was performed as previously described [21]. Briefly, 786-O Cells were seeded on glass coverslips and cultured overnight, then cells were fixed in 4% formaldehyde and subsequently permeabilized with 0.2% Triton X-100, blocked with 5% bovine serum albumin, and incubated with primary antibody at 4 °C overnight, followed by incubation with TRITC conjugated secondary antibodies for 1 h, and stained with DAPI. Finally, images were taken under a fluorescence microscope.

RNA extract, reverse transcription-PCR, and qRT-PCR

RNA was extracted using TRIzol (Invitrogen) and cDNA was synthesized using the HiScript 1st Strand cDNA Synthesis Kit (Vazyme Biotech, Nanjing, China). Real-time PCR was carried out on ABI-7500 using UltraSYBR One-Step RT-qPCR Kit (Vazyme Biotech, Nanjing, China). The primers using for quantitative RT-PCR analysis are listed as follows:

5′-AAGGTCGGAGTCAACGGATTTG-3′ (forward), and 5′-CCATGGGTGGAATCATATTGGAA-3′ (reverse) for GAPDH; 5′- CTCGCTTCGGCAGCACA -3′ (forward), and 5′- AACGCTTCACGAATTTGCGT-3′ (reverse) for U6, 5′- AGTAAGAAGACTCCCGAGGGC-3′ (forward), and 5′-TTACGTTCCACCTGCGTCTC-3′ (reverse) for PinX1, 5′-TCCTTCCCTGTCTGTCTCC -3′ (forward), and 5′- GAC CTAGAAAGCCAGAATAAGA -3′ (reverse) for P1 5′- CTG TCGGGTCTGTCCACCT -3′ (forward), and 5′- CGTATA GTGATCTCCTTGGGTG -3′ (reverse) for P2, 5′- GGTCCC TGATGAGGAAGG -3′ (forward), and 5′- GCAAGGTCG GTTCTACGG -3′ (reverse) for P3, 5′- AGTTGTAAATGA CCCAAAGAAG -3′ (forward), and 5′- TAGCCAACCATC AGAGCC -3′ (reverse) for P4, 5′- GGAGGGATGTCCTGA TGC -3′ (forward), and 5′- CGGTTCCTTTCTCGCAG-3′ (reverse) for P5.

Luciferase reporter assay

The promoter sequence of miR-125a-3p (− 2000 to 0 bp) was cloned to the pGL4.20 vector (Promega) at the upstream of the luciferase sequence by abm company. The miR-125a-Luc and Renilla and PinX1/Control vectors were co-transiently transfected into 293T cells using Lipofectamine 2000. 48 h later, the cells were lysed and the firefly luciferase (Fluc) and Renilla luciferase (Rluc) activities were measured using the Dual Luciferase Reporter Assay System (Promega). The Rluc activity was used for normalization.

Chromatin immunoprecipitation assay

The chromatin immunoprecipitation (ChIP) assay was performed as described previously [22].

miRNA microarray

The expression of miRNAs was determined using Arraystar Human miRNA Microarray (Aksomics Biotech). The sample preparation and microarray hybridization were performed based on the manufacturer's standard protocols.

Animal work

786-O and ACHN cells expressing the control or PinX1 shRNA were mixed with matrigel and were subcutaneously injected into the flanks of 6-week-old nude male mice. 7 days later, mice were killed, and tumors were excised for further analyzing. 786-O cells expressing the control or overexpression were subcutaneously injected into the tail veins of 6-week-old male BALB/c nu/nu mice (Beijing Vital River Laboratory Animal Technology Co., Ltd). For bioluminescence imaging, mice were injected i.p. with 100 mg/kg D-luciferin before imaging. Following anesthesia, images were collected using the Night OWL II LB983 (Berthold Technologies, Bad Wildbad, Germany). Animal experiments were approved by the Animal Care and Use Committee at Xuzhou Medical University. Animal experiments were performed as described previously.

Statistical analysis

Statistical analyses were carried out using SPSS 20.0 software (SPSS Inc., Chicago, IL, USA) and GraphPad Prism 7. The association between miR-125a-3p staining and the clinicopathologic parameters of the RCC patients were evaluated by a χ^2 test. The Kaplan–Meier method and log-rank test were used to evaluate the correlation between miR-125a-3p expression and RCC patient survival. The unpaired t test was used to determine the statistical significance of differences between groups. Data were presented as mean ± SD. $p < 0.05$ was considered statistically significant.

Results

PinX1 represses renal cancer angiogenesis in vitro and in vivo

In our previous study, PinX1 was less expressed in RCC tissues than in normal renal tissues, thereby leading to unfavorable outcomes in patients with RCC. Furthermore, PinX1 inhibited the migration and invasion of RCC in vitro [11]. Considering that angiogenesis is important for tumor growth and metastasis, we further explored the role of PinX1 in angiogenesis in this present study. To further investigate the molecular functions of PinX1 in RCC, we silenced PinX1 in 786-O and ACHN cell lines by using siRNA. Western blot assays showed that PinX1 was silenced in these two cell lines (Fig. 1a). Furthermore, we analyzed the expression of VEGF, which was elevated when PinX1 was knocked down in 786-O and ACHN cells (Fig. 1a). Then, tube formation assays were performed in vitro by using the condition medium collected from PinX1 knockdown cells. Consequently, the average number of complete tubular structures formed by HUVECs and collected from PinX1 knockdown cells significantly increased compared with those of the controls (Fig. 1b, c).

Furthermore, to investigate the effect of PinX1 on angiogenesis in vivo, we injected subcutaneously the PinX1 knockdown 786-O/ACHN and control cells mixed with matrigel into nude mice separately. Then, neovessel formation was examined 1 week later. Visual detection revealed that PinX1 knockdown cells enhanced the neovessels compared with the control (Fig. 1d). PinX1 knockdown promoted renal cancer cell growth in vivo, and the tumor diameter formed by PinX1 knockdown cells was considerably larger than that of control cells (Fig. 1e). The IHC assay further revealed that PinX1 expression was significantly reduced, and the expression levels of VEGF and CD31 were dramatically increased in tumors formed by the PinX1 knockdown cells (Fig. 1f–h). In addition, the CD31 staining showed that the microvessel densities were significantly increased in the tumors upon PinX1 knockdown (Fig. 1i). PinX1 suppressed tumor angiogenesis, thereby suggesting that PinX1 plays an important role in tumor progression.

PinX1 represses VEGF expression through activating the miR-125a-3p transcription

To further explore the potential mechanism of PinX1 in regulating tumor angiogenesis, we performed a miRNA microarray assay. Gene signature analysis of these cohorts revealed that seven miRNAs were 1.5-fold upregulated ($P < 0.05$), and 14 miRNAs were 1.5-fold downregulated ($P < 0.05$) during PinX1 knockdown (Supplementary Table S1). Among the significantly changed miRNAs, miR-125a-3p dramatically decreased when PinX1 was knocked down (Fig. 2a). The following real-time PCR assays also identified that miR-125a-3p was significantly reduced in the PinX1 knockdown cells (Fig. 2b). Then, TargetScan, miRDB, and miRanda tools were used to analyze the binding site of mir-125a-3p in VEGF. mir-125-3p could bind to the 3′UTR of VEGF mRNA (Fig. 2c). To further investigate whether mir-125a-3p could affect the expression of VEGF in PinX1 overexpressed or knockdown cells, we used the mir-125a-3p mimic and inhibitor to assess the effects of mir-125a-3p on VEGF expression. Western blot results showed that mir-125a-3p overexpression reduced the expression of VEGF induced by PinX1 knockdown in 786-O and ACHN cells (Fig. 2d). Moreover, inhibition of mir-125a-3p by mir-125a-3p inhibitor partly rescued VEGF expression (Fig. 2e). Therefore, PinX1 regulates VEGF expression depending on mir-125a-3p expression in renal cancer cells.

Next, to study whether PinX1 could regulate mir-125a-3p at the transcription level, we performed luciferase report assays and chromatin immunoprecipitation assays (CHIP). First, the promoter region (−2000 bp to +0 bp) of mir-125a was cloned to the luciferase report vector. Second, the vectors were co-transfected with PinX1 and Renilla vectors to 786-O cells. After 48 h, luciferase activity was detected, and PinX1 increased mir-125a promoter activity in a dose-dependent manner (Fig. 2f). Furthermore, our CHIP assays were performed to analyze the binding region of PinX1 to mir-125a promoter. Data showed that PinX1 could bind to the promoter region (−498 bp to −412 bp) of mir-125a (Fig. 2g). Therefore, PinX1 promoted mir-125a expression through the transcription activation of mir-125a.

miR-125a-3p functions as a mediator of PinX1-mediated renal cancer angiogenesis

In this study, PinX1 played an important role in renal cancer angiogenesis. To further test the role of mir-125a-3p in PinX1-mediated renal cancer angiogenesis, we used the ELISA assays to detect the secretion of VEGF, which regulates cell angiogenesis. PinX1 knockdown promoted the secretion of VEGF in 786-O and ACHN cells, whereas the re-expression of mir-125a-3p using the mir-125a-3p mimic in PinX1 knockdown 780-O and ACHN cells partly reduced VEGF secretion (Fig. 3a, b). Moreover, inhibition of mir-125-3p in 786-O and ACHN $PinX1^{OE}$ cells increased VEGF secretion (Fig. 3c, d). Finally, to reveal the role of mir-125a-3p in PinX1 repressed angiogenesis,

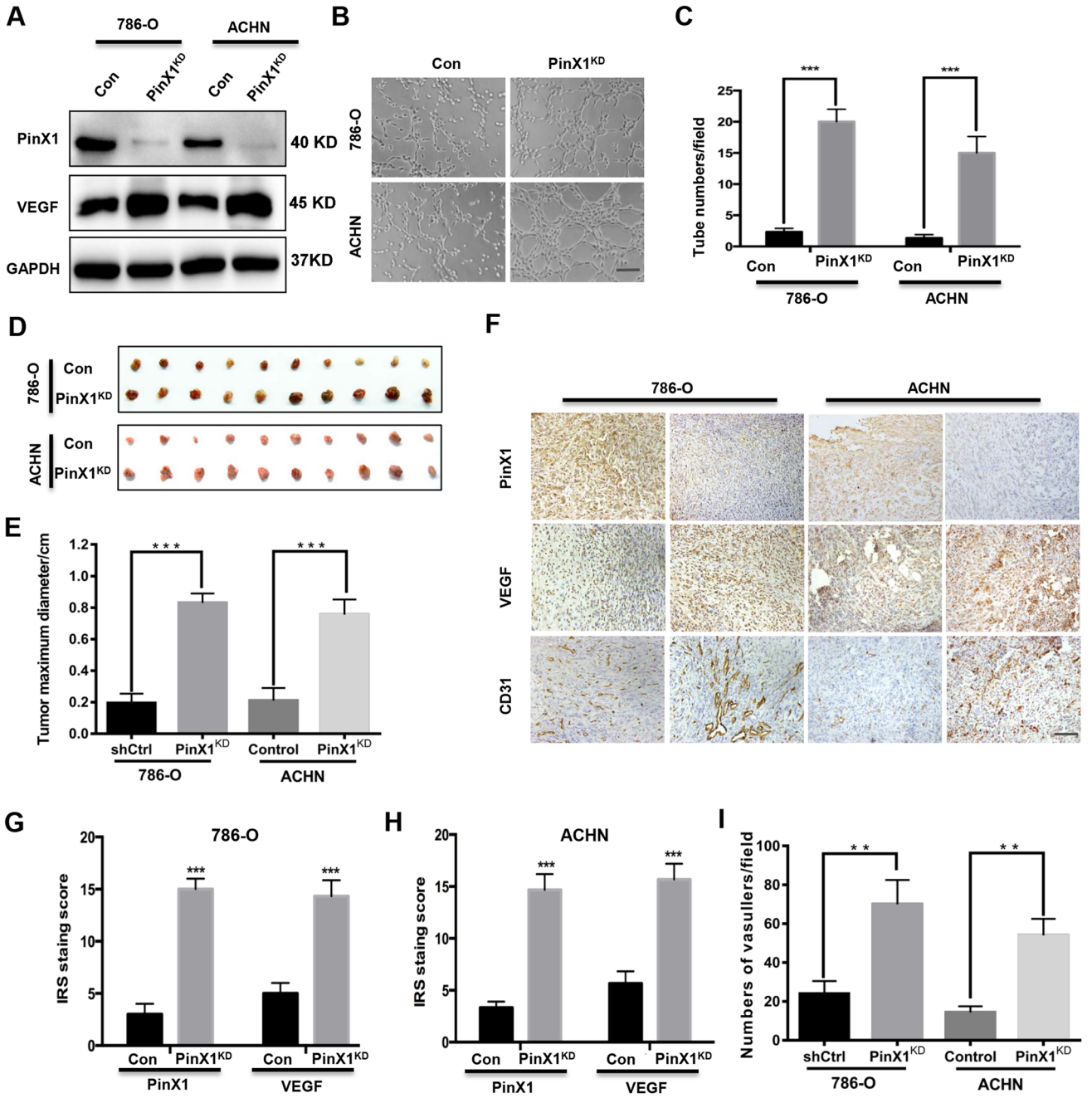

Fig. 1 PinX1 represses renal cancer angiogenesis in vitro and in vivo. **a** Western blot analysis of PinX1 and VEGF protein expression in PinX1 KD 786-O and ACHN renal cancer cell lines, GAPDH was used as a loading control. **b**, **c** PinX1 negatively regulated tube formation. Numbers of complete tubular structures formed by HUVECs were counted for ± PinX1 KD in 786-O and ACHN cells. Scale Bar 50 μm. Data are presented as the mean ± SD for experiments in triplicate. **d** Photographs of matrigel plugs with 786-O and ACHN cells ± PinX1 KD excised from mice after 7 days of growth in vivo. **e** Diameters of the tumors formed by 786-O and ACHN cells ± PinX1 KD. **f** IHC detection of PinX1, VEGF, and CD31 in xenograft tumors. **g**, **h** Quantification of PinX1 and VEGF IHC staining in the xenograft tumors. **i** Quantification of microvessel densities in the xenograft tumors. Scale Bar 50 μm. Statistical analysis was performed using unpaired t-tests. All statistical tests were two-sided. $^{**}p < 0.01$, $^{***}p < 0.001$

we performed tube formation assays in vitro following the guidelines described before [23]; mir-125a-3p overexpression partly reduced the tube numbers formed by HUVECs (Fig. 3e). Taken together, PinX1 might regulate cancer angiogenesis via the mir-125a-3p/VEGF signaling pathway.

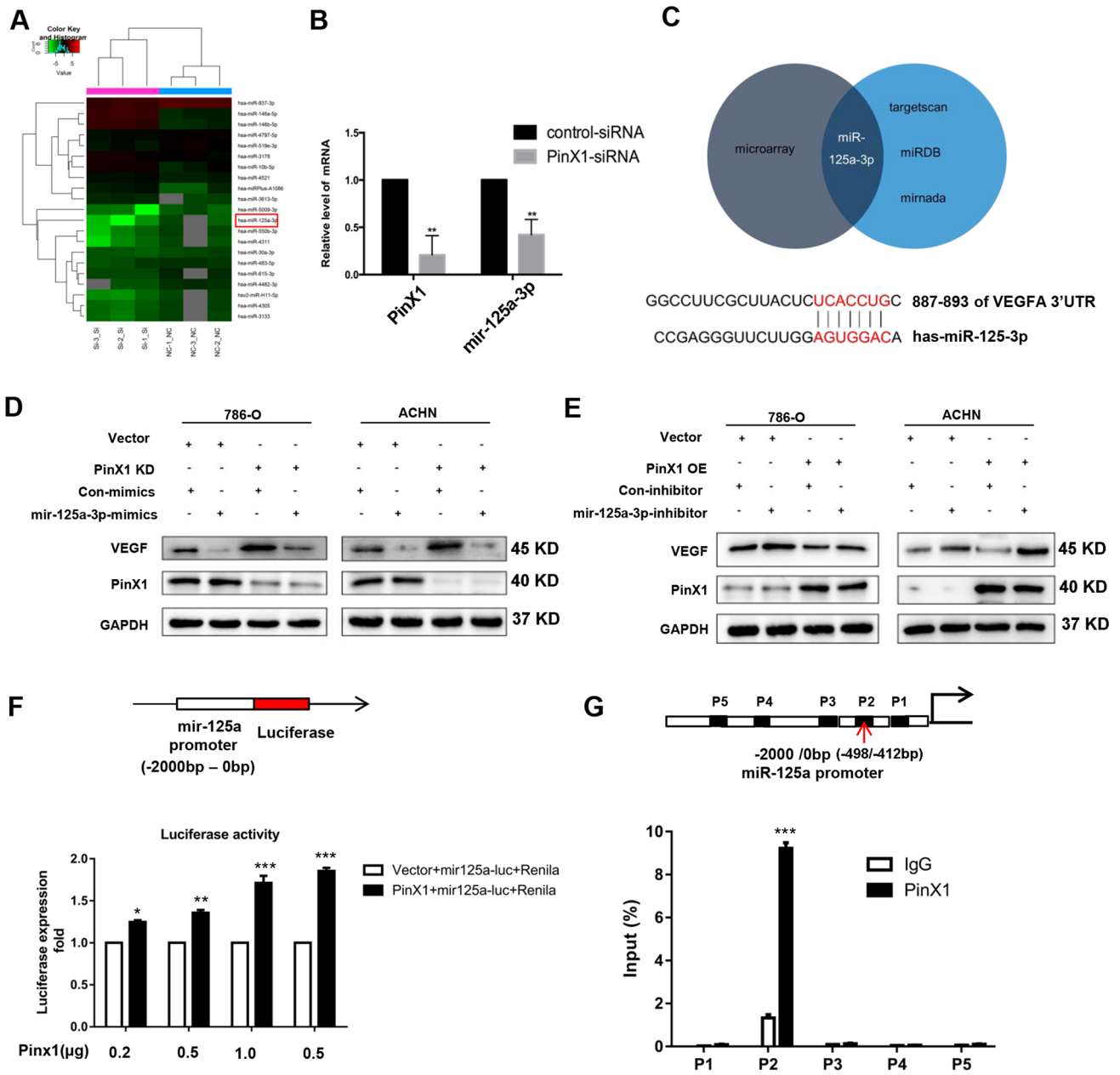

Fig. 2 PinX1 represses VEGF expression through activating miR-125a-3p transcription. **a** Hot map of the different expressions of miRNAs in 786-O cell ± PinX1 KD data using miRNA microarray data. **b** Detection of the miR-125a-3p expression in 786-O cell ± PinX1 KD using Real-time PCR. Values were normalized against U6 from three independent experiments and are presented as mean ± SD. **c** miRNA database from TargetScan, miRDB, and miRanda all showed VEGF was the potential target of mir-125a-3p. **d** 786-O and ACHN cells ± PinX1 KD were co-transfected with miR-125a-mimics or control-mimics and assessed by Western blot for VEGF expression. **d** 786-O and ACHN cells ± PinX1 OE were co-transfected with miR-125a-inhibitor or control-inhibitor and assessed by Western blot for VEGF expression. **e** Relative miR-125a-3p promoter Luc activity in different doses of PinX1 transfection was detected by the Dual Luciferase Reporter Assay System. **f** ChIP-qPCR analysis of PinX1 binding at P1, P2, P3, P4, and P5 loci. Mean ± standard deviation of triplicate experiments are shown. *$p < 0.05$, **$p < 0.01$, ***$p < 0.001$

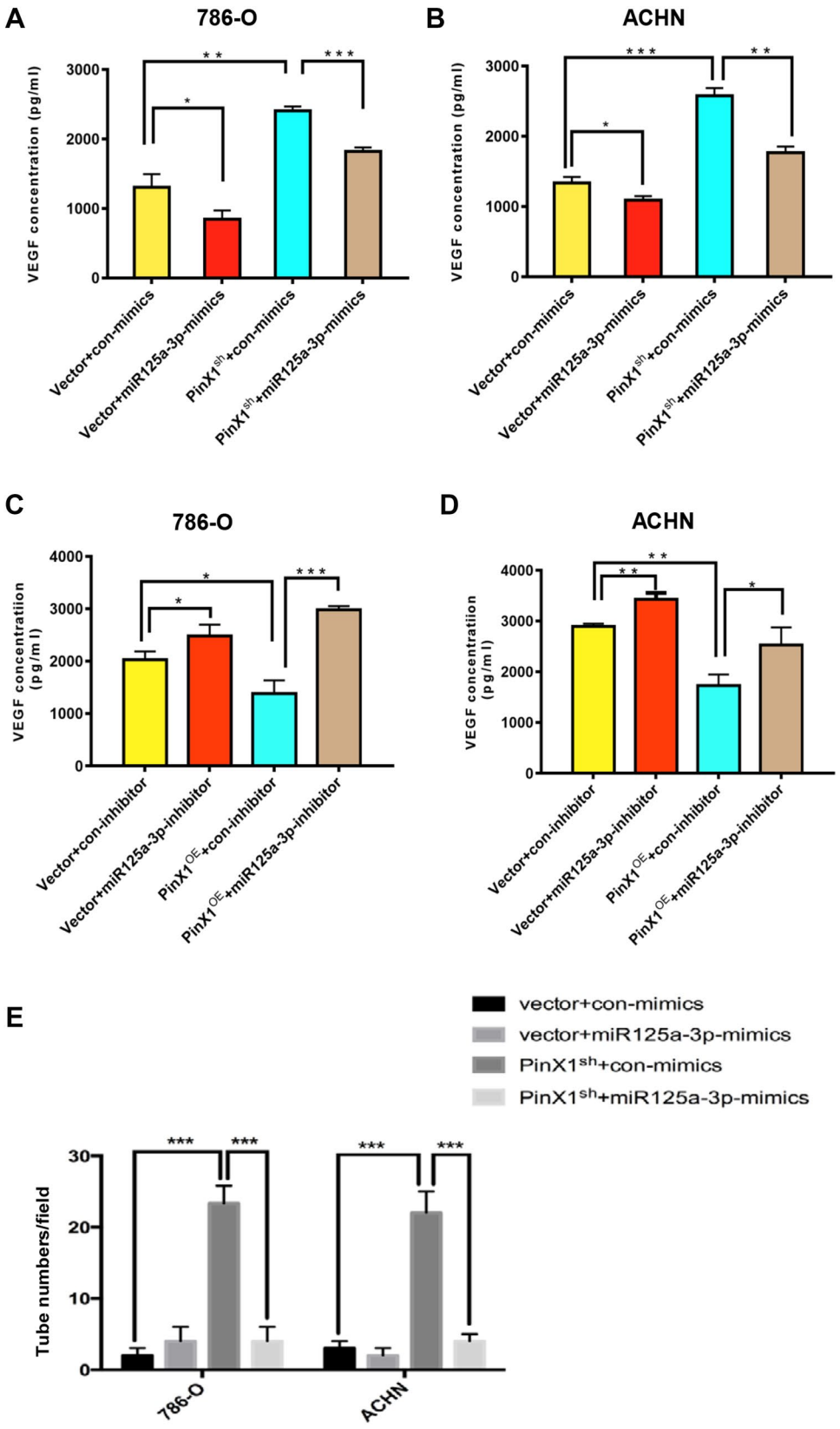

Fig. 3 miR-125a-3p functions as a mediator of PinX1 mediated renal cancer angiogenesis. **a**, **b** ELISA assays were used to detect the secretion of VEGF in 786-O and ACHN cells ± PinX1 KD that co-transfected with miR-125a-mimics or control-mimics. **c**, **d** ELISA assays were used to detect the secretion of VEGF in 786-O and ACHN cells ± PinX1 OE co-transfected with miR-125a-inhibitor or control-inhibitor. **e** Numbers of complete tubular structures formed by HUVECs were counted for ± PinX1 KD in 786-O and ACHN cells that co-transfected with miR-125a-mimics or control-mimics. Mean ± standard deviation of triplicate experiments are shown. $^{*}p < 0.05$, $^{**}p < 0.01$, $^{***}p < 0.001$

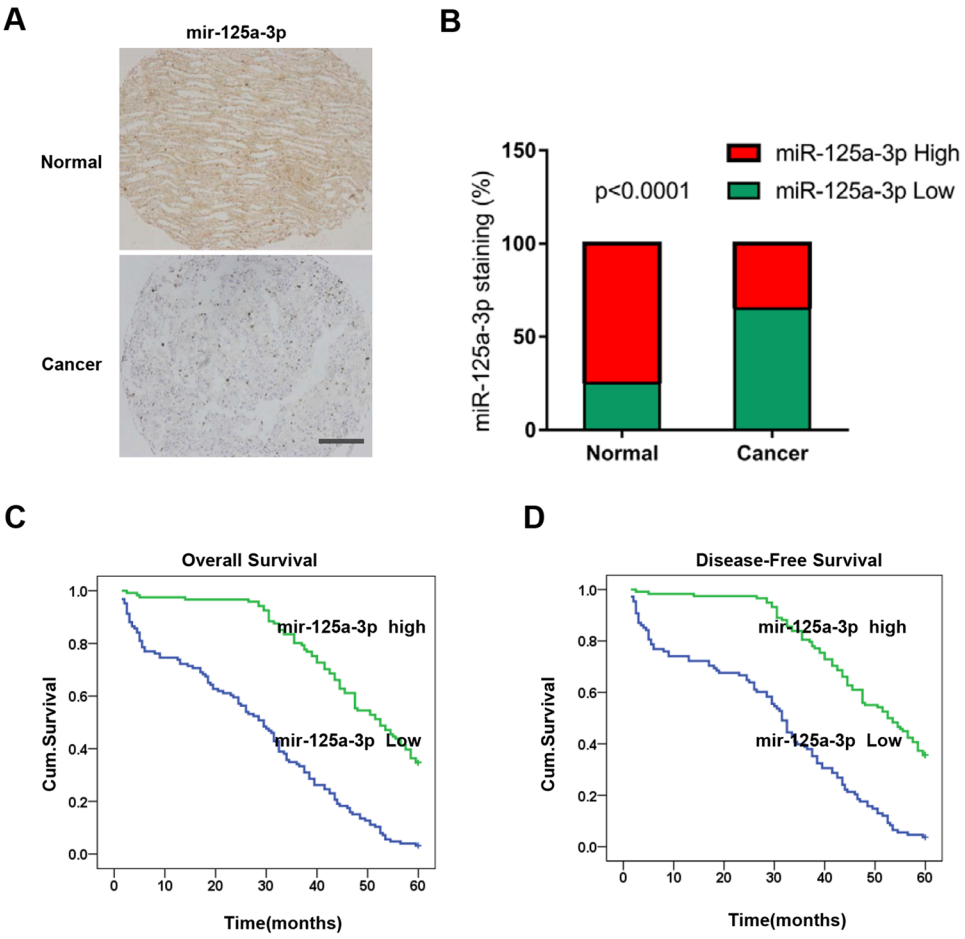

Fig. 4 Low miR-125a-3p is expressed in RCC patients and is correlated with poor survival of RCC patients. **a** Representative ISH images of miR-125a-3p in paired adjacent non-cancerous tissue and renal cancer tissues in RCC patients. Scale Bar 25 μm. **b** miR-125a-3p staining status in non-cancerous tissue and renal cancer tissues in RCC patients. **c** Kaplan–Meier survival curves depicting overall survival ($n=247$, $p<0.001$) stratified by mir-125a-3p staining in RCC tissues. **d** Kaplan–Meier survival curves depicting disease-specific survival of patients with RCC ($n=226$, $p<0.001$) stratified by mir-125a-3p staining in RCC tissues

Low miR-125a-3p is expressed and correlates with the clinicopathological parameters in patients with RCC

PinX1 expression was decreased in RCC tissues, and low PinX1 expression correlated with the depth of invasion, lymph node metastasis, and advanced TNM stage, as well as with the worse overall survival (OS) and disease-specific survival (DFS) in patients with RCC [9]. Considering that mir-125a-3p could be activated by PinX1, ISH was performed to calculate the correlation of mir-125a-3p expression with the clinicopathological parameters of patients with RCC by using tissue microarray (TMA). First, we used a TMA slide containing 75 pairs of RCC tumor tissues and relative adjacent non-tumor tissues to calculate the miR-125a-3p expression. miR-125a-3p was more expressed in normal renal tissues than in RCC tissues (Fig. 4a, b). To analyze the correlation of miR-125a-3p expression with the clinicopathological characteristics of RCC, we used TMAs containing 307 renal cancer tissues to perform ISH to analyze miR-125-3p expression. The above-mentioned correlation was then analyzed (Table 1). Compared with miR-125a-3p expression in histology stages I and II, the expression was dramatically decreased in stages III and IV ($p<0.001$). In addition, low mir-125a-3p expression positively correlated with the depth of invasion ($p=0.002$), lymph node metastasis ($p=0.004$), and tumor diameter ($p=0.003$).

The impact of miR-125a-3p expression on the OS and DFS in patients with RCC was evaluated by Kaplan–Meier survival analysis. Low miR-125a-3p levels correlated with poor OS ($p<0.001$, log-rank test, Fig. 4c) and DFS ($p<0.001$, log-rank test, Fig. 4d). Thus, miR-125a-3p may be a good prognostic factor for OS and DFS.

To further examine whether miR-125a-3p expression was an independent prognostic factor for RCC, we used univariate and multivariate Cox regression analysis models to confirm the prognostic value of miR-125a-3p expression in RCC. According to univariate Cox regression analysis, miR-125a-3p expression was a significant prognostic factor for the OS (HR 3.752, 95% CI 2.791–5.045) and DFS (HR 3.351, 95% CI 2.595–4.805) of patients with RCC (Table 2). In multivariate Cox regression analysis, miR-125-3p expression was also an independent prognostic marker for both OS (HR 3.277, 95% CI 2.326–4.476, $p<0.001$) and DFS (HR 3.103, 95% CI 2.209–4.361, $p<0.001$) in patients with RCC (Table 3).

Table 1 Relationship between mir-125a-3p expression and clinicopathological features of renal cancer patients

Variables	mir-125a-3p expression (n = 307 cases)		
	Low (%)	High (%)	p^a
All patients	166 (100)	141 (100)	
Age (years)			0.422
≤ 56	84 (50)	64 (45)	
> 56	82 (50)	77 (55)	
Gender			0.467
Males	107 (64)	97 (69)	
Females	59 (36)	44 (31)	
Depth of invasion			0.002
T1/T2	124 (75)	125 (89)	
T3/T4	42 (25)	16 (11)	
Lymph node metastasis			0.004
N0	145 (87)	136 (96)	
N1/N2/N3	21 (13)	5 (4)	
Distant metastasis			0.755
M0	138 (83)	120 (85)	
M1	28 (17)	21 (15)	
TNM stage			< 0.001
I/II	93 (56)	107 (76)	
III/IV	73 (44)	34 (24)	
Tumor diameter			0.003
< 7 cm	117 (70)	120 (85)	
≥ 7 cm	49 (30)	21 (15)	

[a]Two -sided Fisher's exact tests

Ectopic overexpression of PinX1 represses the epithelial–mesenchymal transition (EMT) program in renal cancer cells

EMT progress can be repressed by mir-125a-3p [24]. Thus, we investigated whether PinX1 plays a role in EMT program. To study the role of PinX1 in EMT, we overexpressed PinX1 in 786-O and ACHN cells (Fig. 5a) and detected the EMT makers in PinX1-overexpressed cells by using Western blot. Consequently, PinX1 overexpression increased the epithelial makers, namely, E-cadherin, occludin, and β-catenin, and decreased the mesenchymal makers, namely, N-cadherin, vimentin, and fibronectin, in both 786-O and ACHN cells (Fig. 5b). Our immunofluorescence assays also showed that PinX1 overexpression repressed the expression of mesenchymal makers, namely, N-cadherin and vimentin (Fig. 5c). Therefore, PinX1 may be a novel EMT repressor in renal cancer.

PinX1 functions as a suppressor in RCC metastasis in vivo

In this study, PinX1 repressed VEGF expression and cell angiogenesis. Given that angiogenesis is essential for cancer metastasis [25], we investigated the role of PinX1 in RCC metastasis in vivo. The 786-O-Luc-Ctrl, 786-O-Luc-PinX1^{KD}, and 786-O-Luc-PinX1^{OE} cells were injected into the tail veins of nude mice separately. Strikingly, 786-O-Luc-PinX1^{KD} cells effectively metastasized to the lung region of nude mice in 4 weeks, whereas 786-O-Luc-PinX1^{OE} cells ineffectively metastasized to the lung of nude mice, in contrast with the MCF7-Vector cells, as illustrated by the bioluminescence imaging (Fig. 6a, b). Furthermore, we calculated the mice's survival status. PinX1^{KD} decreased the survival rates, whereas PinX1^{OE} increased them (Fig. 6c). Therefore, PinX1 was a repressor of RCC metastasis.

Discussion

PinX1 is a functional gene in human chromosome 8p23 [7]. PinX1 plays an important role as a tumor suppressor in various human cancers, including breast cancer, lung cancer, colon cancer, and renal cancer [5, 11, 26, 27]. However, the

Table 2 Univariate Cox regression analysis of miR-125-3p expression and clinicopathologic variables predicting the survival of renal cancer patients

Variables[a]	Overall survival		Disease-specific survival	
	HR (95% CI)	*p*	HR (95% CI)	*p*
mir-125-3p	3.752 (2.791–5.045)	< 0.001	3.351 (2.595–4.805)	< 0.001
Age	0.936 (0.709–1.234)	0.637	0.949 (0.709–1.272)	0.728
Gender	0.824 (0.619–1.097)	0.184	0.836 (0.618–1.131)	0.245
TNM stage	0.411 (0.299–0.564)	< 0.001	0.397 (0.285–0.554)	< 0.001
LNM	0.328 (0.182–0.583)	< 0.001	1.174 (0.291–4.732)	0.822
Tumor diameter	0.597 (0.425–0.838)	0.003	0.646 (0.446–0.935)	0.021
Depth of invasion	0.664 (0.472–0.934)	0.019	0.713 (0.492–1.032)	0.073

HR hazard ratio, *CI* confidence interval, *LNM* lymph node metastasis

[a]mir-125: low versus high; Age: ≤ 56 versus > 56; Gender: male versus female; LNM: N0 versus N1, N2, N3; Depth of invasion: T1-T2 versus T3-T4; Distant metastasis: M0 versus M1; TNM stage was ranked as I–II versus III–IV; Tumor diameter: < 7 cm versus ≥ 7 cm

Table 3 Multivariate Cox regression analysis of miR-125-3p expression on 5-year overall and disease-specific survival of 307 renal cancer patients

Variable*	Overall survival			Disease-specific survival		
	Hazard ratio	95% CI†	*p**	Hazard ratio	95% CI†	*p**
mir-125a-3p	3.227	2.326–4.476	< 0.001	3.103	2.209–4.361	< 0.001
Age	1.097	0.819–1.470	0.533	1.075	0.793–1.458	0.640
Gender	1.108	0.821–1.494	0.503	1.098	0.803–1.501	0.558
Tumor size	1.386	0.955–2.010	0.085	1.376	0.929–2.037	0.111
TNM stage	1.490	1.061–2.090	0.021	1.506	1.055–2.149	0.024

*Coding of variables: Cancer was coded as 1 (negative), and 2 (positive). Age was coded as 1 (≤ 56 years), and 2 (> 56 years). Gender was coded as 1 (male), and 2 (female).Tumor size was coded as 1 (< 7 cm), and 2 (≥ 7 cm). TNM stage was coded as 1 (I–II), and 2 (III–IV)

†*CI* confidence interval

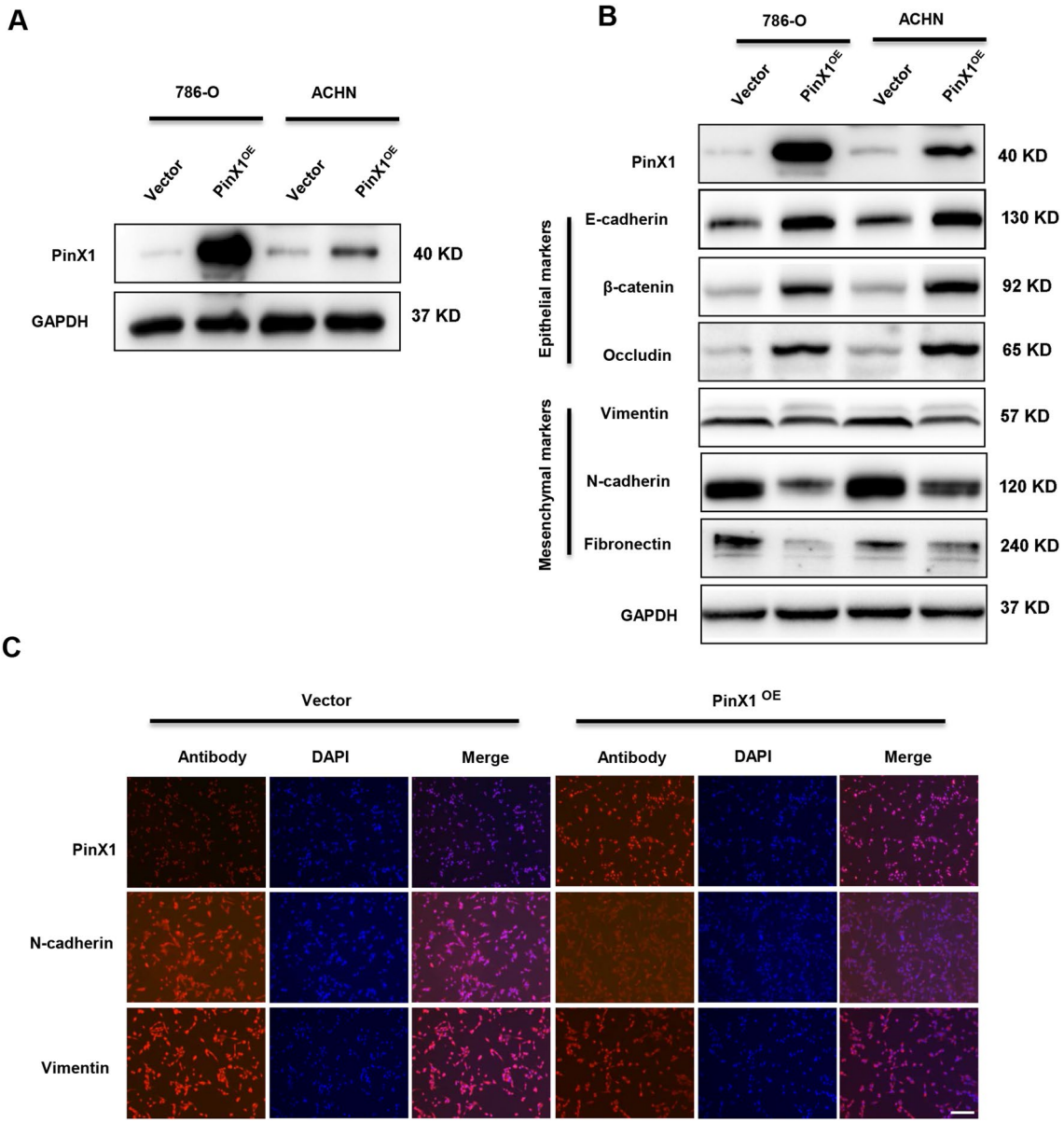

Fig. 5 Ectopic overexpression of PinX1 represses EMT program in renal cancer cells. **a** Ectopic expression of PinX1 expression was confirmed by western blot in 786-O and ACHN cells. **b** Western blots analysis of the epithelial (E-cadherin, β-catenin, and Occludin) and mesenchymal markers (Fibronectin, N-cadherin, and Vimentin) in 786-O and ACHN cells ± PinX1 OE. **c** Immunofluorescence staining for PinX1, N-cadherin, and Vimentin in 786-O cells ± PinX1 OE. Scale Bar 100 μm

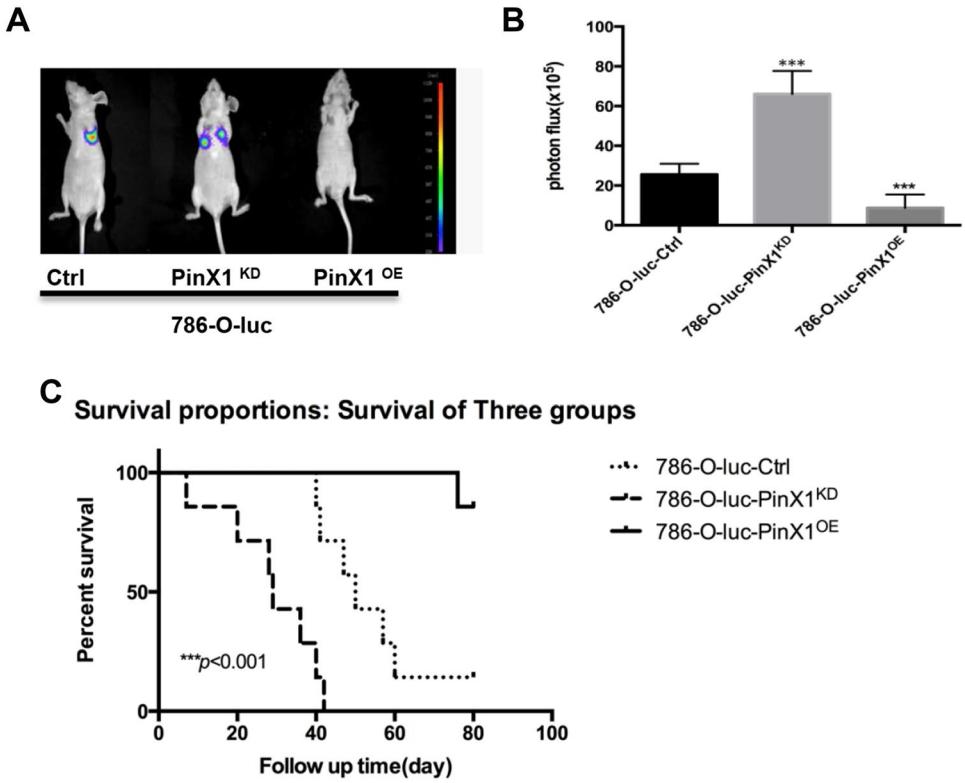

Fig. 6 PinX1 functions as a suppressor in renal cancer tumor metastasis in vivo. **a** Representative bioluminescence images of lung metastases in mice via tail vein injection of indicated cells. **b** The metastases were quantified by measuring the photo flux. Data are presented as the mean ± standard deviation, $***p < 0.001$. **c** Kaplan–Meier survival curves depicting overall survival of the mice with injection of 786-O control, PinX1 KD, and PinX1 OE cells

molecular mechanism and functions underlying the role of PinX1 in renal cancer progression remain unclear and need to be explored.

Our initial observations focused on the abnormal expression deficiency of PinX1 in renal tumor tissues compared with the normal tissues, and we showed that PinX1 suppressed renal cancer invasion and metastasis via the NF-κB/MMP2 pathway [11]. In previous works, the functions of PinX1 were mainly in proliferation, repression, and invasion. In this present study, we focused on the tumor repressor role of PinX1, and we found that PinX1 represses renal cancer angiogenesis in vitro and in vivo by regulating VEGF. VEGF is a key regulator of angiogenesis and plays an essential role in angiogenesis and tumor metastasis; angiogenesis is also essential in tumorigenesis and metastasis [28, 29]; angiostatic treatments have been used widely in tumor treatment [30]. PinX1 may inhibit tumor proliferation and invasion by repressing angiogenesis.

To further understand the molecular mechanism of PinX1 in renal cancer angiogenesis, we obtained the gene microarray to determine the downstream molecules of PinX1 in renal cancer. Surprisingly, PinX1 promoted the expression level of miR-125a-3p, which is a tumor suppressor of multiple oncogenes, including VEGF, CDK3, FUT5/6, and ERBB2/3 [13, 31–33]. PinX1 could also promote miR-125a-3p expression by activating miR-125a-3p transcription. Moreover, miR-125a-3p was essential for VEGF expression in $PinX1^{KD}$ or $PinX1^{OE}$ renal cells.

We first revealed that miR-125a-3p expression was significantly higher in the adjacent normal renal tissues compared with RCC tissues, thereby suggesting that miR-125a-3p is a biomarker in RCC. Multivariate Cox regression analysis indicated that low miR-125a-3p expression was an independent prognostic factor for OS and DFS. Therefore, miR-125a-3p can be used as a prognostic biomarker and a novel therapeutic target in RCC.

EMT and mesenchymal–epithelial transition (MET) program are two opposite reversible processes and are accompanied by massive changes, such as cell proliferation, differentiation, migration, and adhesion, in cell behavior [34]. In this present study, we showed that ectopic overexpression of PinX1 in 786-O and ACHN cells induced MET accompanied with gaining of epithelial marker expression and losing of mesenchymal marker expression. The repressive role of PinX1 in EMT is consistent with previous reports in which PinX1 functions as a tumor suppressor and inhibits cell migration and invasion properties [5, 6, 35]. Additionally, $PinX1^{OE}$ repressed RCC metastasis and promoted mouse survival rate in lung metastasis model.

Conclusions

In conclusion, PinX1 functions as a repressor in tumor angiogenesis and metastasis in renal cancer. We discovered a new molecular mechanism of PinX1 in which

PinX1 transcriptionally activated mir-125a-3p expression, thereby inhibiting the expression of VEGF. Moreover, the loss of mir-125a-3p expression was detected in patients with RCC. Thus, miR-125a-3p can be used as a prognostic biomarker and a novel therapeutic target in RCC.

Acknowledgements We thank the department of pathology of the Affiliated Hospital of Xuzhou Medical University for the assistance of collecting the patients' samples.

Author contributions PFH, JNZ, and JB provided study concept and design. PFH, HLL, HMY, FC, and SFC collected and analyzed the data. PFH, HLL, and HMY interpreted the data. PFH, HLL, HMY, FC, and SFC performed the experiments. HLL and HMY collected the patients' samples. PFH and JB wrote the manuscript. All authors approved the final version of manuscript.

Funding This work was supported by Grants from the National Natural Science Foundation of China (Nos. 81874183, 81602533, 81672845, and 81872304), the Jiangsu Provincial Key Medical Discipline, and the Project of Invigorating Health Care through Science, Technology and Education (Nos. ZDXKA2016014, ZDRCC2016009), and the Qing Lan Project.

Compliance with ethical standards

Conflict of interest The authors declare no conflict of interest.

Ethical approval This study was conducted in compliance with the Declaration of Helsinki. Informed consent was obtained from all subjects. The ethics approval statements for human subjects were provided by the Ethnic Committee of the Affiliated Hospital of Xuzhou Medical University. The ethics approval statements for animal work were provided by the Institutional Animal Care and Use Committee of Xuzhou Medical University.

References

1. Siegel RL, Miller KD, Jemal A (2018) Cancer statistics. CA 68:7–30
2. Banik SSR, Counter CM (2004) Characterization of interactions between PinX1 and human telomerase Subunits hTERT and hTR. J Biol Chem 279:51745–51748
3. Johnson FB (2011) PinX1 the tail on the chromosome. J Clin Invest 121:1242–1244
4. Chen YL, Capeyrou R, Humbert O, Mouffok S, Kadri YA, Lebaron S et al (2014) The telomerase inhibitor Gno1p/PINX1 activates the helicase Prp43p during ribosome biogenesis. Nucleic Acids Res 42:7330–7345
5. Shi ML, Cao MH, Song J, Liu QH, Li HL, Meng F et al (2015) PinX1 inhibits the invasion and metastasis of human breast cancer via suppressing NF-kappa B/MMP-9 signaling pathway. Mol Cancer 14(1):66
6. Zhou XZ, Huang P, Shi R, Lee TH, Lu G, Zhang Z et al (2011) The telomerase inhibitor PinX1 is a major haploinsufficient tumor suppressor essential for chromosome stability in mice. J Clin Investig 121:1266–1282
7. Kondo T, Oue N, Mitani Y, Kuniyasu H, Noguchi T, Kuraoka K et al (2005) Loss of heterozygosity and histone hypoacetylation of the PINX1 gene are associated with reduced expression in gastric carcinoma. Oncogene 24:157–164
8. Cai MY, Zhang B, He WP, Yang GF, Rao HL, Rao ZY et al (2010) Decreased expression of PinX1 protein is correlated with tumor development and is a new independent poor prognostic factor in ovarian carcinoma. Cancer Sci 101:1543–1549
9. Liu JY, Qian D, He LR, Li YH, Liao YJ, Mai SJ et al (2013) PinX1 suppresses bladder urothelial carcinoma cell proliferation via the inhibition of telomerase activity and p16/cyclin D1 pathway. Mol Cancer 12:148
10. Zhang L, Jiang Y, Zheng Y, Zeng Y, Yang Z, Huang G et al (2011) Selective killing of Burkitt's lymphoma cells by mBAFF-targeted delivery of PinX1. Leukemia 25:331–340
11. Li HL, Han L, Chen HR, Meng F, Liu QH, Pan ZQ et al (2015) PinX1 serves as a potential prognostic indicator for clear cell renal cell carcinoma and inhibits its invasion and metastasis by suppressing MMP-2 via NF-kappa B-dependent transcription. Oncotarget 6:21406–21420
12. Zhang B, Bai YX, Ma HH, Feng F, Jin R, Wang ZL et al (2009) Silencing PinX1 compromises telomere length maintenance as well as tumorigenicity in telomerase-positive human cancer cells. Cancer Res 69:75–83
13. Scott GK, Goga A, Bhaumik D, Berger CE, Sullivan CS, Benz CC (2007) Coordinate suppression of ERBB2 and ERBB3 by enforced expression of micro-RNA miR-125a or miR-125b. J Biol Chem 282:1479–1486
14. Guan Y, Yao HL, Zheng ZH, Qiu GR, Sun KL (2011) MiR-125b targets BCL3 and suppresses ovarian cancer proliferation. Int J Cancer 128:2274–2283
15. Huang L, Luo JH, Cai QQ, Pan QH, Zeng H, Guo ZH et al (2011) MicroRNA-125b suppresses the development of bladder cancer by targeting E2F3. Int J Cancer 128:1758–1769
16. Liang LH, Wong CM, Ying QA, Fan DNY, Huang SL, Ding J et al (2010) MicroRNA-125b suppressesed human liver cancer cell proliferation and metastasis by directly targeting oncogene LIN28B. Hepatology 52:1731–1740
17. Liang X, Shi H, Yang L, Qiu C, Lin S, Qi Y et al (2017) Inhibition of polypyrimidine tract-binding protein 3 induces apoptosis and cell cycle arrest, and enhances the cytotoxicity of 5- fluorouracil in gastric cancer cells. Br J Cancer 116:903–911
18. Saharinen P, Eklund L, Pulkki K, Bono P, Alitalo K (2011) VEGF and angiopoietin signaling in tumor angiogenesis and metastasis. Trends Mol Med 17:347–362
19. Smits M, Wurdinger T, van het Hof B, Drexhage JAR, Geerts D, Wesseling P et al (2012) Myc-associated zinc finger protein (MAZ) is regulated by miR-125b and mediates VEGF-induced angiogenesis in glioblastoma. Faseb J 26:2639–2647
20. Bi Q, Tang SH, Xia L, Du R, Fan R, Gao LC et al (2012) Ectopic expression of MiR-125a inhibits the proliferation and metastasis of hepatocellular carcinoma by targeting MMP11 and VEGF. PLoS ONE 7(6):e40169
21. Hou P, Li L, Chen F, Chen Y, Liu H, Li J et al (2018) PTBP3-mediated regulation of ZEB1 mRNA stability promotes epithelial-mesenchymal transition in breast cancer. Can Res 78:387–398
22. Hou PF, Jiang T, Chen F, Shi PC, Li HQ, Bai J et al (2018) KIF4A facilitates cell proliferation via induction of p21-mediated cell cycle progression and promotes metastasis in colorectal cancer. Cell Death Dis 9(5):477
23. Nowak-Sliwinska P, Alitalo K, Allen E, Anisimov A, Aplin AC, Auerbach R et al (2018) Consensus guidelines for the use and interpretation of angiogenesis assays. Angiogenesis 21:425–532
24. Liu G, Ji L, Ke M, Ou Z, Tang N, Li Y (2018) miR-125a-3p is responsible for chemosensitivity in PDAC by inhibiting epithelial-mesenchymal transition via Fyn. Biomed Pharmacother 106:523–531
25. Carmeliet P, Jain RK (2011) Principles and mechanisms of vessel normalization for cancer and other angiogenic diseases. Nat Rev Drug Discov 10:417–427

26. Tian XP, Jin XH, Li M, Huang WJ, Xie D, Zhang JX (2017) The depletion of PinX1 involved in the tumorigenesis of non-small cell lung cancer promotes cell proliferation via p15/cyclin D1 pathway. Mol Cancer 16(1):74
27. Jiang T, Li HQ, Jiang RR, Li HL, Hou PF, Chen YS et al (2018) Pin2/TRF1-binding protein x1 inhibits colorectal cancer cell migration and invasion in vitro and metastasis in vivo via the nuclear factor-B signaling pathway. Oncol Rep 40:1533–1544
28. Folkman J (2002) Role of angiogenesis in tumor growth and metastasis. Semin Oncol 29:15–18
29. Ferrara N (2005) The role of VEGF in the regulation of physiological and pathological angiogenesis. Birkhäuser, Basel, pp 209–231
30. Nowak-Sliwinska P, van Beijnum JR, Huijbers EJM, Gasull PC, Mans L, Bex A et al (2019) Oncofoetal insulin receptor isoform A marks the tumour endothelium; an underestimated pathway during tumour angiogenesis and angiostatic treatment. Br J Cancer 120:218–228
31. Zheng L, Meng X, Li X, Zhang Y, Li C, Xiang C et al (2018) miR-125a-3p inhibits ERalpha transactivation and overrides tamoxifen resistance by targeting CDK3 in estrogen receptor-positive breast cancer. FASEB J 32:588–600
32. Liang L, Gao C, Li Y, Sun M, Xu J, Li H et al (2017) miR-125a-3p/FUT5-FUT6 axis mediates colorectal cancer cell proliferation, migration, invasion and pathological angiogenesis via PI3 K-Akt pathway. Cell Death Dis 8:e2968
33. Bi Q, Tang S, Xia L, Du R, Fan R, Gao L et al (2012) Ectopic expression of MiR-125a inhibits the proliferation and metastasis of hepatocellular carcinoma by targeting MMP11 and VEGF. PLoS ONE 7:e40169
34. Hanahan D, Weinberg RA (2011) Hallmarks of cancer: the next generation. Cell 144:646–674
35. Tian XP, Qian D, He LR, Huang H, Mai SJ, Li CP et al (2014) The telomere/telomerase binding factor PinX1 regulates paclitaxel sensitivity depending on spindle assembly checkpoint in human cervical squamous cell carcinomas. Cancer Lett 353:104–114